

University of Veterinary Medicine Budapest
Department of Anatomy and Histology



**3D reconstruction and analyses of the anatomy of an
elephant's foot using CT and MRI**

By: Shannon Rück

Supervisors:

Dr. Reinitz László Zoltán, assistant professor

Dr. Petneházy Örs, honoured docent and research veterinarian,
Medicopus Nonprofit Kft, Kaposvári Egyetem

Budapest, 2020

Table of contents

| | | |
|--------|--|----|
| 1. | Introduction..... | 2 |
| 2. | Literature review | 4 |
| 2.1. | Overview of the anatomical structures of elephant’s feet | 4 |
| 2.2. | Anatomy of the forelimb (starting at the <i>antebrachium</i>) | 4 |
| 2.2.1. | Bones and joints of the forelimb..... | 4 |
| 2.2.2. | Vessels and nerves of the forelimb | 6 |
| 2.3. | Anatomy of the hindlimb (starting at the crus) | 7 |
| 2.3.1. | Bones and joints of the hindlimb | 7 |
| 2.3.2. | Vessels and nerves of the hindlimb | 8 |
| 2.4. | Special feature: the “sixth” toe and its role | 8 |
| 3. | Materials and methods | 10 |
| 3.1. | Visualisation of the bones with the 3D Slicer program | 12 |
| 3.2. | Visualisation of the vessels with the 3D Slicer program | 13 |
| 3.3. | Visualisation of the joints with the 3D Slicer program..... | 15 |
| 4. | Results..... | 16 |
| 4.1. | Results of the bone reconstructions..... | 16 |
| 4.2. | Results of the vessel reconstructions..... | 22 |
| 4.3. | Results of the joint reconstructions | 26 |
| 5. | Discussion and conclusion..... | 27 |
| 6. | Summary | 32 |
| 7. | Összefoglaló..... | 33 |
| 8. | Bibliography | 34 |
| 9. | Acknowledgements..... | 36 |

1. Introduction

Elephants, known best as the largest still living terrestrial mammals, belong to the family *Elephantidae*, the last non-extinct family in the order *Proboscidea*. Today three species are still extant: the Asian elephant (*Elephas maximus*), the African bush elephant (*Loxodonta africana*) and the African forest elephant (*Loxodonta cyclotis*). As herbivorous, non-ruminant mammals, wild elephants occur in Southeast Asia and parts of Africa.

The average shoulder height/body weight in adult elephants is 260 cm/3.000 kg for females and 320 cm/6.000 kg for males in *Loxodonta africana* and 240 cm/2.700 kg for females and 275 cm/4.000 kg for males in *Elephas maximus* (Larramendi, 2016).

The closest extant relatives are the *Sirenia* (sea cows, dugongs and manatees) and the *Hyracoidea* (hyraxes), which are grouped beside the *Proboscidea* in the clade *Paenungulata* (Kellogg et al., 2007).

Records of interactions between elephants and humans exist already since the stone-age, where elephants and extinct relatives were hunted and appeared in various art since then. They were used in battles and wars, being a symbol of power and strength. They were and are still used especially in Asia as working animals, carrying heavy burden for example. Nowadays captive elephants play a role in tourism and are displayed in circuses or zoos (Fowler & Mikota, 2006).

The Red List of the International Union for Conservation of Nature (IUCN) listed African elephants as a vulnerable species, whereas Asian elephants belong to the endangered species with decreasing population numbers (IUCN Red List, 2020).

Elephant's feet play an important role in their overall health status, as their high body weight is supported by them. Foot disorders are quite common problems in captive elephants, which affect more often Asian elephants than African elephants for unknown reasons. Besides the main tasks in elephants' husbandry like feeding and cleaning, a large amount of time has to be dedicated to the soundness of the feet (Fowler & Mikota, 2006; Regnault et al., 2017). According to Csuti et al. (2001), many predisposing factors are known for the development of foot problems such as the lack of exercise, overgrown toenails or soles, hygienic issues and many more. Elephants cover a huge distance per day if allowed, which assures inter alia the essential function of blood circulation. Due to gravity and the extreme sizes it takes more effort for the circulation to lift the blood from the limbs back to the heart, that is why while moving, the so-called "digital cushion" in the elephants' foot

gets pressurized and acts like a pump forcing the blood to flow upwards (Fowler & Mikota, 2006).

Significant amount of literature was found about the bones of elephants, but only few 3D data can be found, which does not include vessels or joint cavities or the vessels and bones in correlation.

The aim of this work is to provide easily accessible anatomical guidance, using modern 3D reconstructions as illustrative models, focusing especially on the skeletal and vascular findings. It will highlight the relationship between these structures to help veterinarians, veterinary students, keepers or other interested persons enhancing their knowledge about this topic. With this we want to help optimizing environmental structures to ensure and maintain the health of these animals, especially under the danger of extinction in the nature and to sustain the species to our best knowledge in captivity.

2. Literature review

2.1. Overview of the anatomical structures of elephant's feet

For the description of the anatomy of elephant's feet the works of Csuti et al. (2001), Fowler & Mikota (2006) and Smuts & Bezuidenhout (1993, 1994) were consulted if not indicated otherwise. For the bones of the digits the paper by Mumby et al. (2015) was also used, as that provides more details on this region.

Although the anatomy of the African (*Loxodonta africana*) and Asian (*Elephas maximus*) elephant's feet shows many commonalities, there are some differences in the number of phalanges and toenails. The following description applies for both species, differences are highlighted.

The roundish forefoot is semidigitigrade (elephants are not only walking on their forelimb's toes solely, they are supported by a surrounding fibroelastic digital cushion) while the slightly smaller and laterally compressed oval shaped hindfoot is semiplantigrade (while walking, the heel is not completely on the ground - as it would be in a plantigrade foot - but also not as high raised as in a foot which is digitigrade).

The forelimbs are slightly longer than the hindlimbs, carrying 60% of the total body weight. This is achieved by the lengthening of the proximal bones of the forelimb, but not the distal ones. The bones of the legs are straight, only little angulation can be found. More precisely, the bones of the metacarpus and metatarsus feature a perpendicular angulation during weight bearing, whereas the phalanges themselves occupy a nearly horizontal position. The limb bones are massive and lack a marrow cavity, which is replaced with cancellous bone. This provides stronger bone material and haematopoiesis concurrently.

2.2. Anatomy of the forelimb (starting at the *antebrachium*)

2.2.1. Bones and joints of the forelimb

The bones of the forelimb are arranged differently than we usually see in most known mammals. The radius is reduced, smaller and shorter than the ulna, which leads to the assumption that the ulna is responsible for most of the weight bearing aspect of the antebrachium. Regarding to Ahasan et al. (2016), the slightly curved radius articulates with its caudal-proximal part with the ulna, then takes a lateral turn over the cranial aspect of the ulna to make its lateral side articulate with the ulnas' medial site at its distal end. There is no interosseous space between the two bones. They are fixed in pronation, which makes it

impossible for elephants to rotate their front limbs. The radius and ulna articulate proximally with the humerus to form the elbow joint and distally with the first row of the carpal bones being part of the carpal joint.

The carpus contains eight bones in total, divided into two rows with four bones each. In the first row from medial to lateral there are the *os carpi radiale*, *os carpi intermedium*, *os carpi ulnare* and the *os carpi accessorium*. The second row consists of *os carpale I, II, III* and *IV* (C-I to C-IV). The radial carpal bone is the most flattened one in the first row, having articulations with the radius proximally, the intermediate carpal bone laterally and with the second and third carpal bones distally. The intermediate carpal bone is wedge-shaped, articulating with both the radius and ulna as well as the ulnar carpal bone laterally and distally with the third carpal bone. The ulnar carpal bone has a slightly triangular shape and has articulations with the ulna proximally, the accessory carpal bone on its palmar side and the fourth carpal bone at its distal aspect. A small elongated area facing the fifth metacarpal bone is also described. The last bone of the first row, the accessory carpal bone, articulates with the ulna and the ulnar carpal bone and shows a tuberos elongated process protruding in caudopalmar direction. The carpal bones I to IV of the second row articulate with their corresponding metacarpal bones (MC-I to MC-V), with *os carpale IV* also having an articulation with *os metacarpale V*. The C-I has a similar flattened shape as the radial carpal bone, being wedge-shaped. C-II has a triangular shape with an additional dull-edged palmar projection; its articulations are found with C-III laterally and proximally with the medial aspect of the radial carpal and the intermediate carpal bone. Next in row is the square-like C-III, which articulates besides of the already mentioned bones with MC-II and MC-III. The last bone of the carpus is C-IV, which communicates with MC-III, MC-IV and MC-V. According to their size, from the largest to the smallest, *os carpale V* is followed by *os carpale III*, *os carpale II* and the smallest is *os carpale I*.

In comparison to other ungulates, the carpus of elephants allows only little abduction (Csuti et al., 2001). In the Asian elephant the synovial layer of the carpal joint inserts on every row of the carpus, fully separating the three carpal joints (*articulatio antebrachio-carpea*, *art. mediocarpea* and *art. carpometacarpeae*).

There are five metacarpal bones, with the third being the largest, followed by the fourth, second, fifth and the first being the smallest (Ahasan et al., 2016). This arrangement is corresponding with the size of the digits themselves as well. Palmar to the *articulatio*

metacarpophalangea each metacarpal bone, except for the first, presents a pair of sesamoid bones. The metacarpal bones articulate with the proximal phalanges next.

Although not externally identifiable, both fore- and hind limb consist of five digits (D-I to D-V) with interspecies differences in the bone numbers. For some of the digits, depending on individuals and the species, protective but not weight bearing toenails are visible on the dorsolateral surface of the foot.

In the majority of Asian elephants five toenails are in each forefoot and four in each hindfoot. African elephants usually show four toenails in each forefoot and three in each hindfoot. Sometimes individual deviations can be seen, bearing less toenails than expected. According to Csuti et al. (2001) the digits II, III and IV have each three phalanges (*phalanx proximalis*, *phalanx media* and *phalanx distalis*) in both species. The following descriptions of the phalanges apply for the fore- and hindfoot equally: the proximal and intermediate phalanges are quadrangular shaped; the distal phalanx has a unique spindle-shaped form with transverse processes on both sides and a single dorsal process. It may not articulate with the intermediate phalanx and is, embedded in soft tissue, attached to a toenail.

In the African elephant, D-I consists of one phalanx and additionally one single sesamoid bone, whereas the D-I of the Asian elephant bears two phalanges and one single sesamoid bone. D-V has two phalanges in both species.

D-I and D-V stand almost perpendicular to the ground, whereas D-II to D-IV incline in an oblique way.

2.2.2. Vessels and nerves of the forelimb

For the description of the forelimb's vessels in the Asian elephant, the work of Csuti et al. (2001) was consulted. For those cases, when the Latin names were not mentioned we used the Veterinary Anatomical Nomenclature (Constantinescu et al., 2012) for the official names of the homologous structures in the household mammals. The median artery (*a. mediana*) goes along with the median vein and nerve at the medial aspect of the *antebrachium* down to the carpus, from that point on it becomes the metacarpal artery (*a. metacarpea*).

A branch of the median artery is the interosseous artery (*a. interossea*), descending to the lateral side of MC-V, continuing as the fifth digital artery. This vessel is homologous with the common interosseous artery (*a. interossea communis*) of the household mammals.

The metacarpal artery flows deep to the metacarpal bones, gives off the first dorsal digital (*a. digitalis dorsalis I.*) artery before it curves ventrolateral forming the deep palmar arch

(*arcus palmaris profundus*). From there metacarpal arteries arise for digits I to V (*aa. metacarpeae dorsales I-V.*). They become palmar digital arteries (*aa. digitales palmares I-V.*), the recurrent branches supplying the carpal joints and the dorsal metacarpal arteries for D-II to D-V, which are continuing further on as the dorsal digital arteries (*aa. digitales dorsales communes I-V.*). Arteries or branches of arteries that supply the digital cushion (*torus digitalis*) were not explicitly mentioned.

The median nerve (*n. medianus*) travels along with the eponymous artery and vein to the carpus. Below the carpal region, it is divided into four terminal branches, namely the palmar digital nerves for D-I to D-IV (*nn. digitales palmares I-IV.*). These accompany the common digital flexor tendon to D-I to D-IV. The palmar digital nerve for D-V is formed by the palmar branch of the ulnar nerve (*n. ulnaris*).

Dorsal digital nerves to D-I to D-III come from the radial nerve (*n. radialis*) and to D-IV and D-V from the dorsal branch of the ulnar nerve, which joined the radial nerve (*n. radialis*).

2.3. Anatomy of the hindlimb (starting at the crus)

2.3.1. Bones and joints of the hindlimb

The tibia and fibula are separate bones in the elephant's hindlimbs.

The tarsus contains seven bones in total, divided into three rows. Calcaneus and talus form the proximal row. The talus has a discoid shape and shows a dorsoplantar compression and articulates with its single *trochlea tali* with the cochlea of the tibia. The calcaneus is the largest bone of the tarsus, its prominent *tuber calcanei* points plantarly. Between the talus and calcaneus there are two articular surfaces. Through the *canalis tarsi* run vessel and nerve for the innervation of the hindlimb. The *os tarsi centrale* is the exclusive bone of the second row. The distal row consists of the wedge-shaped *os tarsi I, II, III* and *IV*. Each of these four tarsal bones have an articulation surface with its corresponding metatarsal bone, with *os tarsi IV* articulating with *os metatarsale V* as well. In the African elephant four individual synovial sacs are identified.

Equally to the metacarpal bones, the third metatarsal bone is the largest and the first metatarsal bone the smallest.

Five digits exist in the hind foot as well, arranged in a tilted position. Except for D-I, every digit presents a pair of sesamoid bones plantar to the corresponding *articulatio metatarsophalangea*. D-III and D-IV are larger than the other ones and bear three phalanges

in both species. In the African elephant, D-I consists only of a single sesamoid bone, whereas in the Asian elephant D-I is formed by one phalanx without a sesamoid bone.

D-II has two phalanges in the African and three phalanges in the Asian elephant. D-V bears in each species two phalanges. A slight axial angulation of the second and fourth digit towards the third digit can be noticed.

2.3.2. Vessels and nerves of the hindlimb

The vessels of the hindlimb are described in an African elephant. Cranial tibial vessel (*a. tibialis cranialis*) flow along the medial part of the cranial tibial muscle, becoming smaller at the tarsus. The caudal tibial artery (*a. tibialis caudalis*) and veins go down dividing into medial and lateral vessels at the calcaneus. Through the tarsal canal the medial branch passes (*a. tarsea perforans*) together with the tibial nerve (*n. tibialis*). The lateral branch however runs craniomedially over MT-V, dividing into a large cutaneous branch and forming the axial and abaxial arteries for D-V.

In the Asian elephant, the tibial artery runs deep to the deep digital flexor at the *tuber calcanei*, dividing into a medial and lateral branch. The medial goes along with the medial plantar nerve down to the digital cushion, where the lateral branch ends as well.

Dorsal digital nerves are formed by the deep peroneal nerve (*n. peroneus profundus*).

2.4. Special feature: the “sixth” toe and its role

The fore- and hind foot feature a unique characteristic in both the Asian and the African elephant, the so called prepollux or prepollex on the forelimb and prehallux on the hindlimb (**Figure 1.**). They were described in Csuti et al. (2001) Fowler & Mikota (2006), Hutchinson et al. (2011), Milller et al. (2008) and Weissengruber et al. (2006).

Anatomically observed, the prepollux is a cone shaped elongated rod in the forefoot which is slightly curved and ends bluntly. It extends distally from *os carpale I* and *os metacarpale I* and attaches to the sole medial to the midline of the foot towards the sole. On MC-I there is a smooth ridge caudomedially as an articulation surface.

The prehallux is mediolaterally flattened with a widened distal end. It acts similarly to the prepollux and extends distally from *os tarsale I* and *os metatarsale I*, attaching to the sole medial to the midline. Articulation surfaces are found on the distal end of T-I in form of a ball- and socket like joint and a ridge on the caudomedial aspect of MT-I.

These so called predigits are assumed to act like real “sixth” digits for further stabilization of the carpal and tarsal joints and redirect some of the pressure load from the digits to the beforementioned joints. They are usually of cartilaginous structure and can become partly or completely ossified over time. Because of their location – palmar medial – they can be referred to as “digit zero” to prevent confusion.

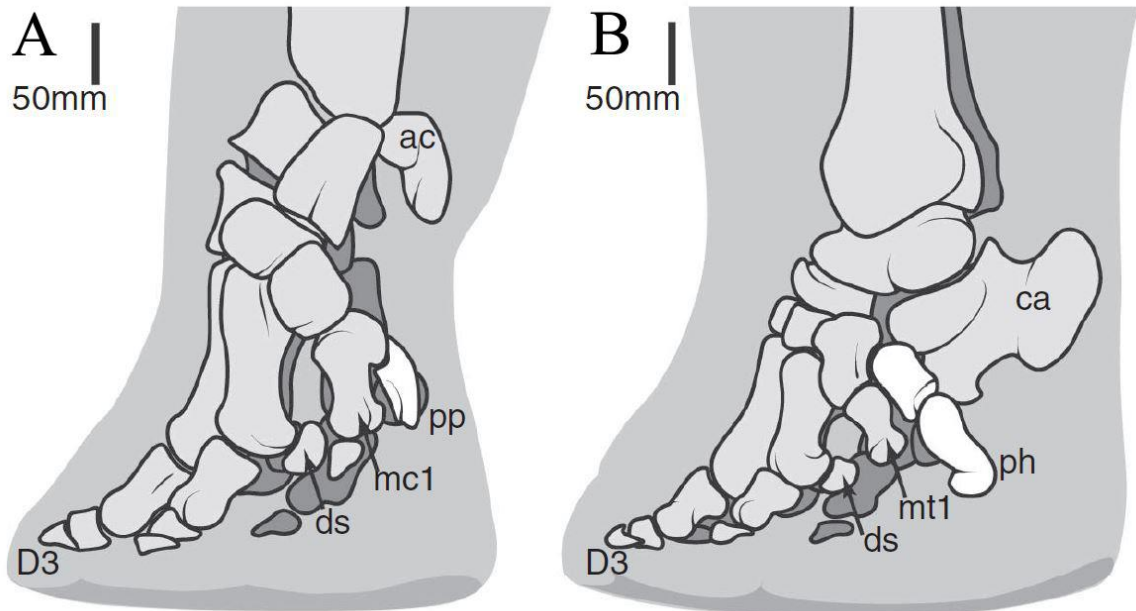


Figure 1.: **A:** prepollux (pp); **B:** prehallux (ph). ac: os carpi accessorium, mc1: os metacarpale I., ds: os sesamoideum proximale, D3: digit III, ca: calcaneus, mt1: os metatarsale I. Hutchinson et al. (2011)

3. Materials and methods

For our investigations we were given the opportunity to use CT and MRI images of a left forelimb and a right hindlimb of a deceased 6-year old female Asian elephant for further investigations. The death was not related to any foot problems, the limbs were in a good condition.

For the preparation of the specimen for the scans, the limbs were cut at the level of the *antebrachium* and crus with a bone saw. Our goal was to gain as much anatomical information we could, therefore we cannulated the median artery with a PVC tube and secured it to prevent any leakage. We were not able to cannulate the cranial tibial artery therefore we missed the chance to reconstruct the vessels of the hindlimb.

After the preparations we placed the specimens on PVC carrying tubes to prevent any movements during transportation between the CT and MR units.

The CT scan (**Figure 2.**) was performed at the Moritz Kaposi Teaching Hospital Dr. József Baka Diagnostic, Radiation Oncology, Research and Teaching Center (Kaposvár, Hungary) with a Siemens Somatom Sensation Cardiac CT (Multislice scanner, Siemens AG, Erlangen, Germany). We completed two separate scanning series. First a native scanning was made from the middle of the antebrachium distal to the sole with the following settings: transverse slices, caudal vision of image, 120 kV, 80 mAs, 0.6 mm slice thickness, 492 mm field of view (FOV) with isotropic voxels and a total number of 2x1600 slices. After that the arteries of the forelimb were filled with 120 ml of Iomeron 400 (iomeprol, Bracco, UK) solution via the cannula placed earlier in the median artery and the scanning was repeated in the same position with the same settings. The hindlimb was scanned native only with the same settings resulting in 1800 transverse slices.

The reconstruction kernel was U40u. The series were saved in DICOM format.

After we completed the CT scan, the specimen was transferred to the MR unit (Siemens Avanto, 1.5T, Siemens AG, Erlangen, Germany) avoiding any movements of the cadaver during transportation.

Transversal, T1-weighted Fast Imaging Low Angle Shot (FLASH) 3D gradient echo sequence was used for acquisition on 4 consecutive regions, covering the entire body. Scan parameters were as follow: TR 8.03 ms, TE 4.78 ms, flip angle: 20, matrix: 320 x 320, FOV 450 mm, slice thickness 1.41 mm (isotropic voxels), NEX 1. The images were reconstructed without gaps and saved in DICOM format.

The obtained data sets were applied to the 3D Slicer program, Version 4.10.2. This program's mainframe was developed over a long period of time with the support from the National Institutes of Health as well as with the help of a worldwide community of developers (Fedorov et al., 2012; Kapur et al., 2016; Kikinis et al., 2014). 3D Slicer is a free and open source software platform, utilizable for medical image informatics, processing of images and visualisation with the aid of 3D models. It is not intended for clinical usage but provides valuable processing tools for research purposes.

After a thoroughly first quality evaluation of the beforementioned data sets the best series from each CT and MRI was chosen for the reconstruction of the bones, vasculature and joint cavities.



Figure 2.: Left: topogram of a left forelimb, dorsal view. Right: topogram of a right hindlimb, latero-plantar view.

3.1. Visualisation of the bones with the 3D Slicer program

The first step was to identify the bones. For that we used the “Threshold” effect of the “Segment Editor” module (**Figure 3.**) as an automatic segmentation. The program recognizes structures of the same intensity range, stains them in the favoured colour and generates a 3D model out of the given data. Afterwards a careful, manual overview of each slice was performed to verify the borders, excess textures were deleted. This procedure was utilized for both the front- and hindlimb.

The next step was the coloration of each single bone or bone group for an even better overview. The principle was the same, but we had to add one segment for every bone we wanted to be stained in a different colour. After selection with the “Grow from seeds” effect we were able to create a multicoloured 3D reconstruction of the limbs (**Figure 4.**).

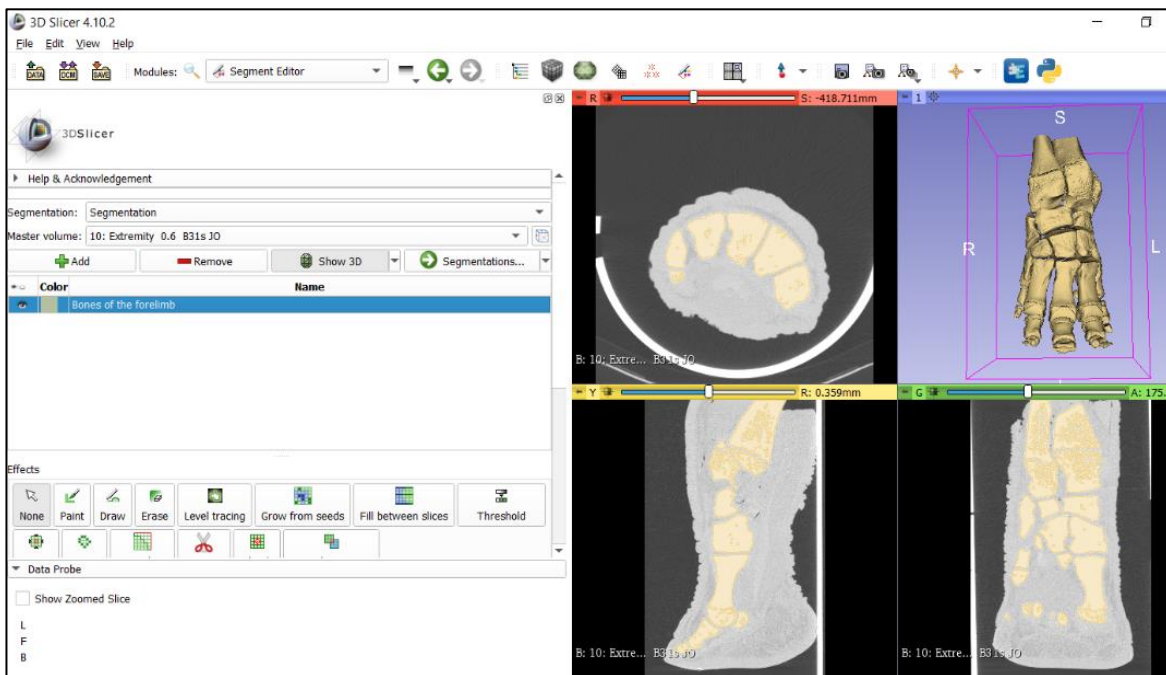


Figure 3.: Screenshot of 3D Slicer; colouring process with the “Threshold” effect.

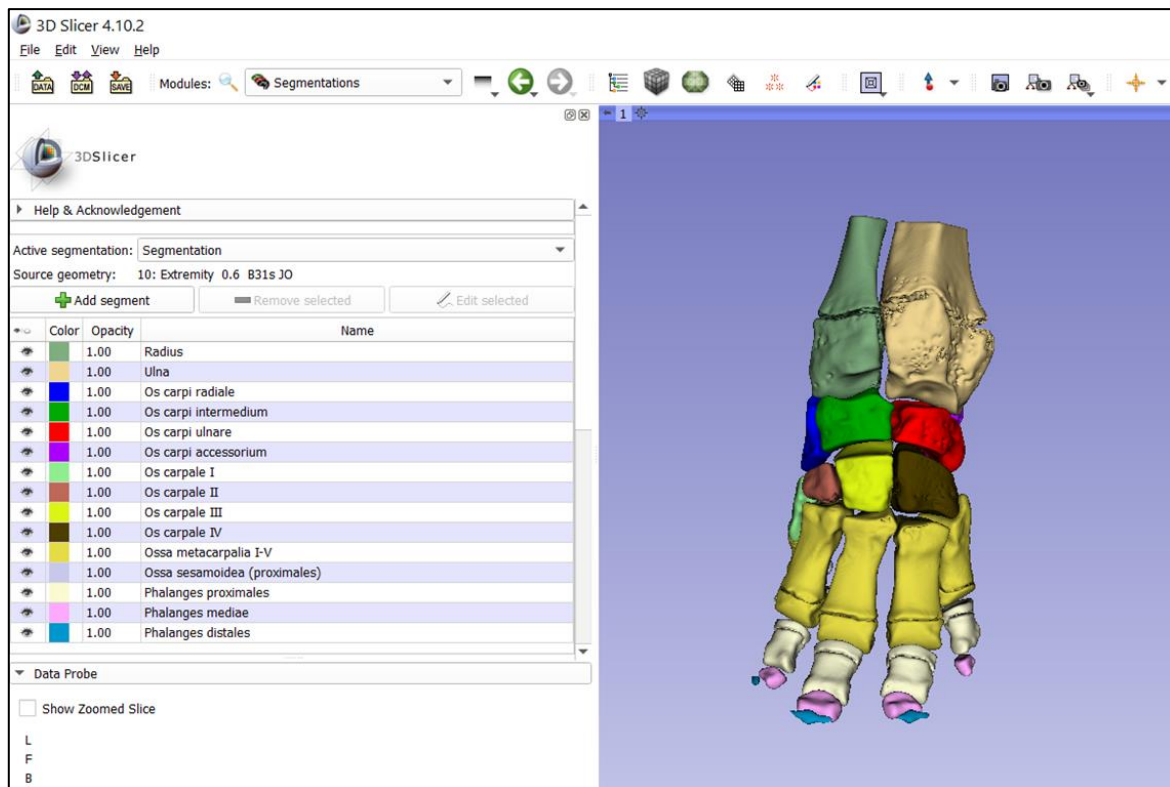


Figure 4.: Screenshot of 3D Slicer; colouring process with the “Grow from seeds” effect.

3.2. Visualisation of the vessels with the 3D Slicer program

The vessels were reconstructed with the “Subtract scalar volumes” module in the 3D Slicer (**Figure 5.**). For this process we needed to load a native sequence and one where the vessels were injected with the iodine contrast medium into the program. It then recognizes the difference between the two sequences, in this case the injected vessels, and is able to subtract them.

We tried to apply this technique for both the fore- and hindlimb, but it was only successful for the first mentioned as described at the scanning protocols.

We continued by using the “Segment editor” as previously to obtain a 3D model for the forelimb’s vessels. A further step was to combine the reconstructed bones with the vessels to see their relationship to each other (**Figure 6.**).

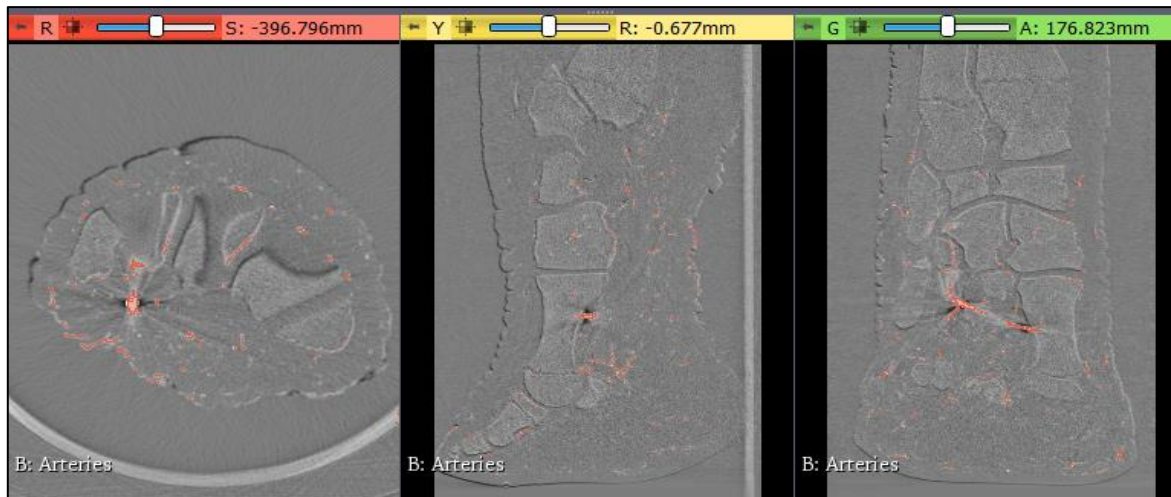


Figure 5.: Screenshot of 3D Slicer; “Subtract scalar volume” with “Threshold” effect.

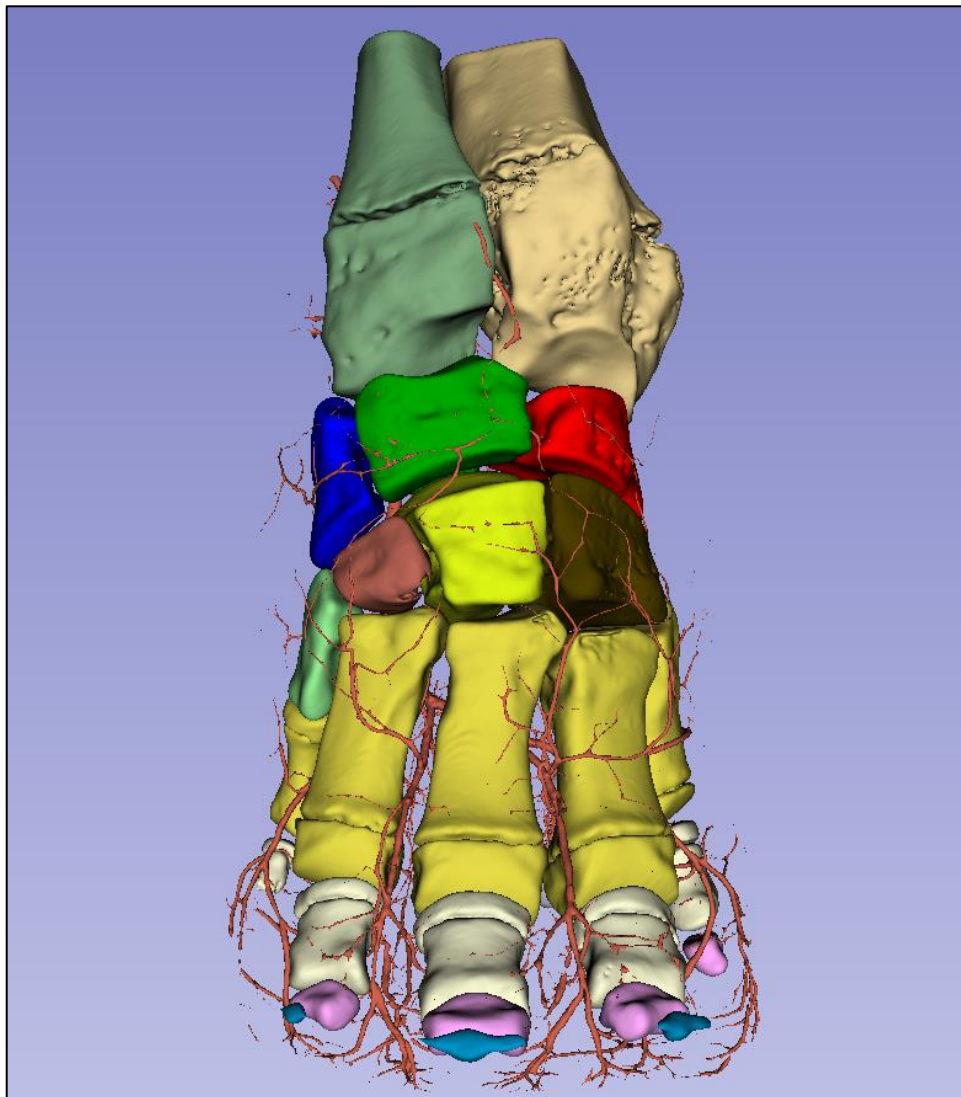


Figure 6.: Screenshot of 3D Slicer; Fused image of the bones and vessels on the forelimb, dorsal view.

3.3. Visualisation of the joints with the 3D Slicer program

For the visualisation of the joints, we used a CT and MRI sequence and fused them in the 3D Slicer with the “Registration” module. Because the CT and MRI images were obtained in slightly different positions due to the usage of two different devices, we had to first align them manually and afterwards with the help of the 3D Slicer module “Transform” so that they are exactly on top of each other (**Figure 7.**). The positioned MRI sequence was then combined with the reconstructed bones and the cartilages were coloured in the “Segment Editor” with the help of the “Threshold” and “Grow from seeds” effects.



Figure 7.: Screenshot of 3D Slicer; Fused MRI and CT images of the left forelimb.

The cartilages of the carpal joint are accentuated with whitish lines.

4. Results

The goal of this study was to identify the bones and vessels found in an elephants' foot and to highlight the peculiarities of this Asian elephants' limbs. Our images, 3D models and a 3D print will illustrate our results with the unique features of this specimen in an easy approachable way.

4.1. Results of the bone reconstructions

We were able to reproduce the native limbs with the help of the 3D Slicer, which gave us the opportunity to determine the quantity of the fore- and hindlimbs' toenails without even the necessity to see the real limbs. The specimen bears five toenails in the front foot and four toenails in the hind foot, which correlates to the usual findings in the Asian elephant. (**Figure 8.**) With the sequences we received from the CT imaging and with the help of the 3D Slicer program multicoloured 3D models were created from the fore- and hindlimb, which can be digitally viewed from every perspective (**Figure 9-10.**).

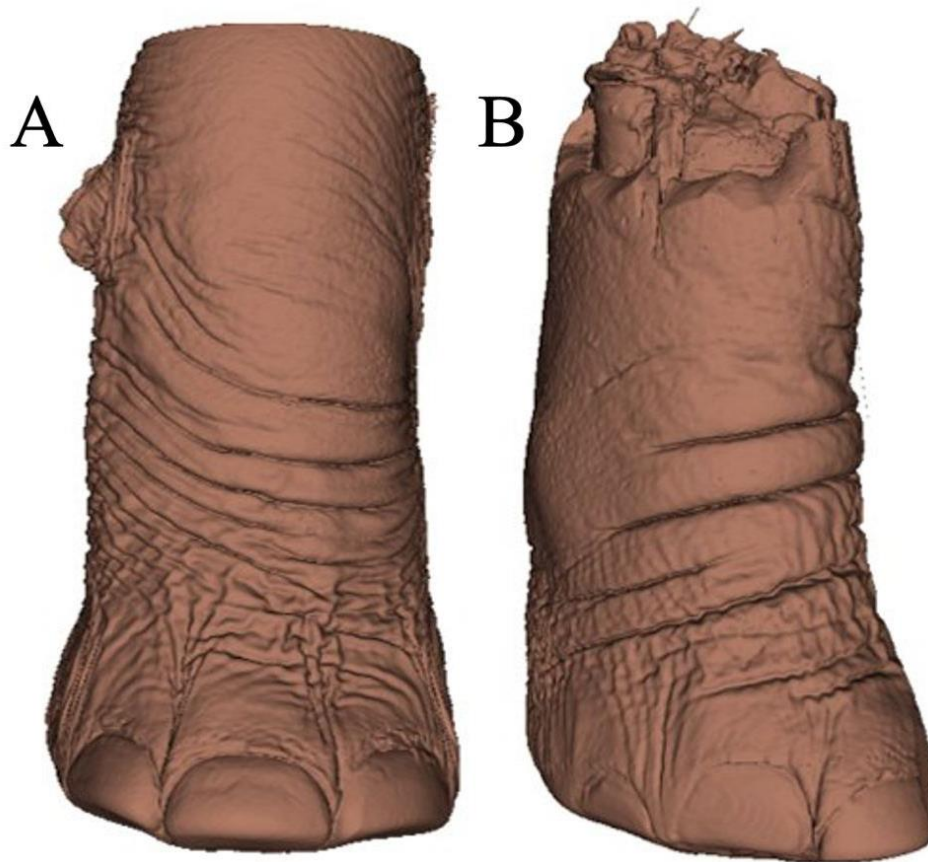


Figure 8.: 3D reconstructions of the fore- and hindlimb. **A:** dorsal view, left forelimb;
B: medial dorsal view, right hindlimb.

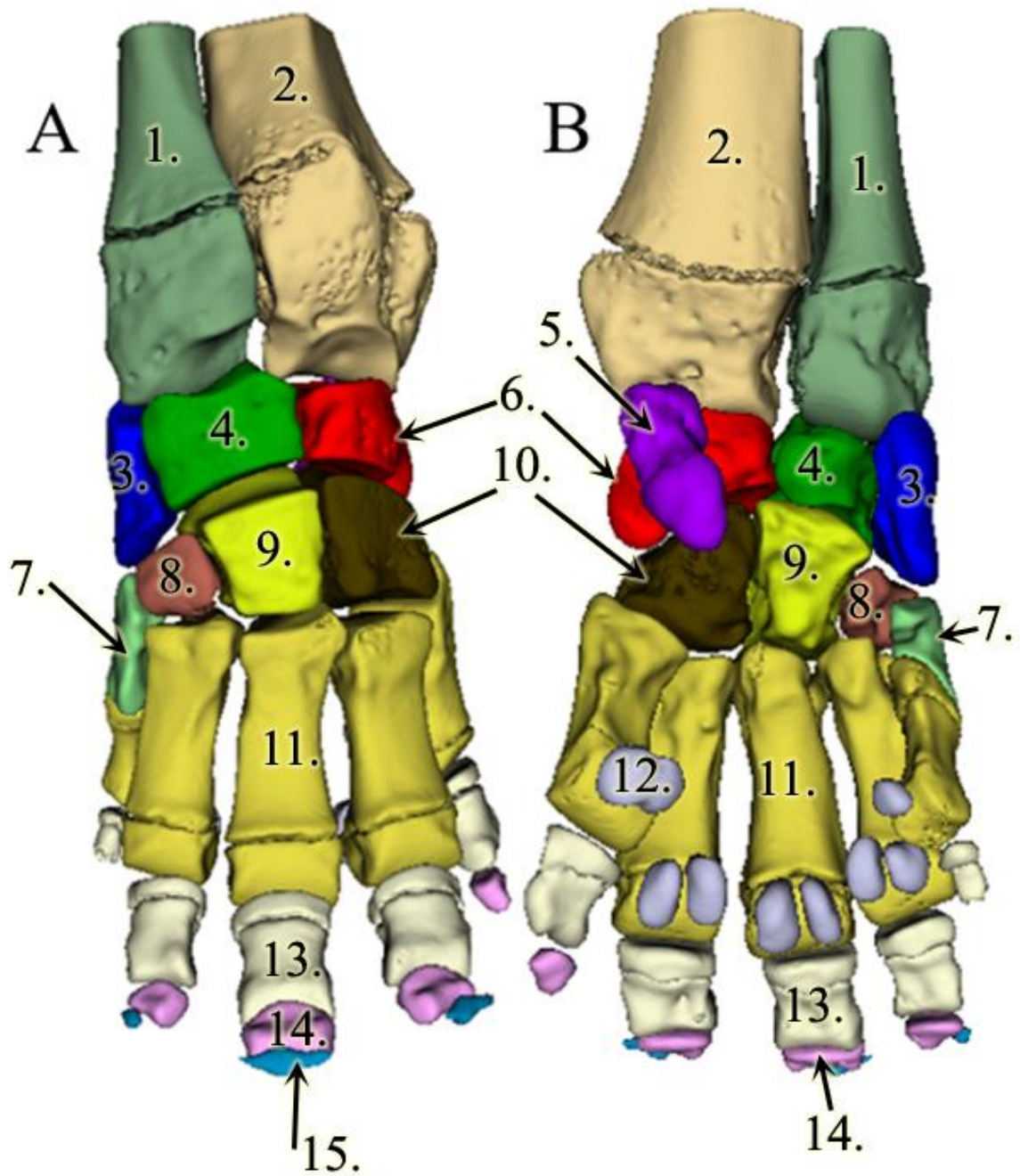


Figure 9.: 3D model of the left forelimb; **A:** dorsal view; **B:** palmar view.

Antebrachium: **1:** radius, **2:** ulna.

Carpus: **3:** os carpi radiale, **4:** os carpi intermedium, **5:** os carpi accessorium (only seen in palmar view), **6:** os carpi ulnare, **7:** os carpale I, **8:** os carpale II, **9:** os carpale III, **10:** os carpale IV.

Metacarpus: **11:** os metacarpale III.

12: ossa sesamoidea proximales (seen in palmar view).

Digiti manus: **13:** phalanx proximalis III, **14:** phalanx media III.,

15: phalanx distalis III.

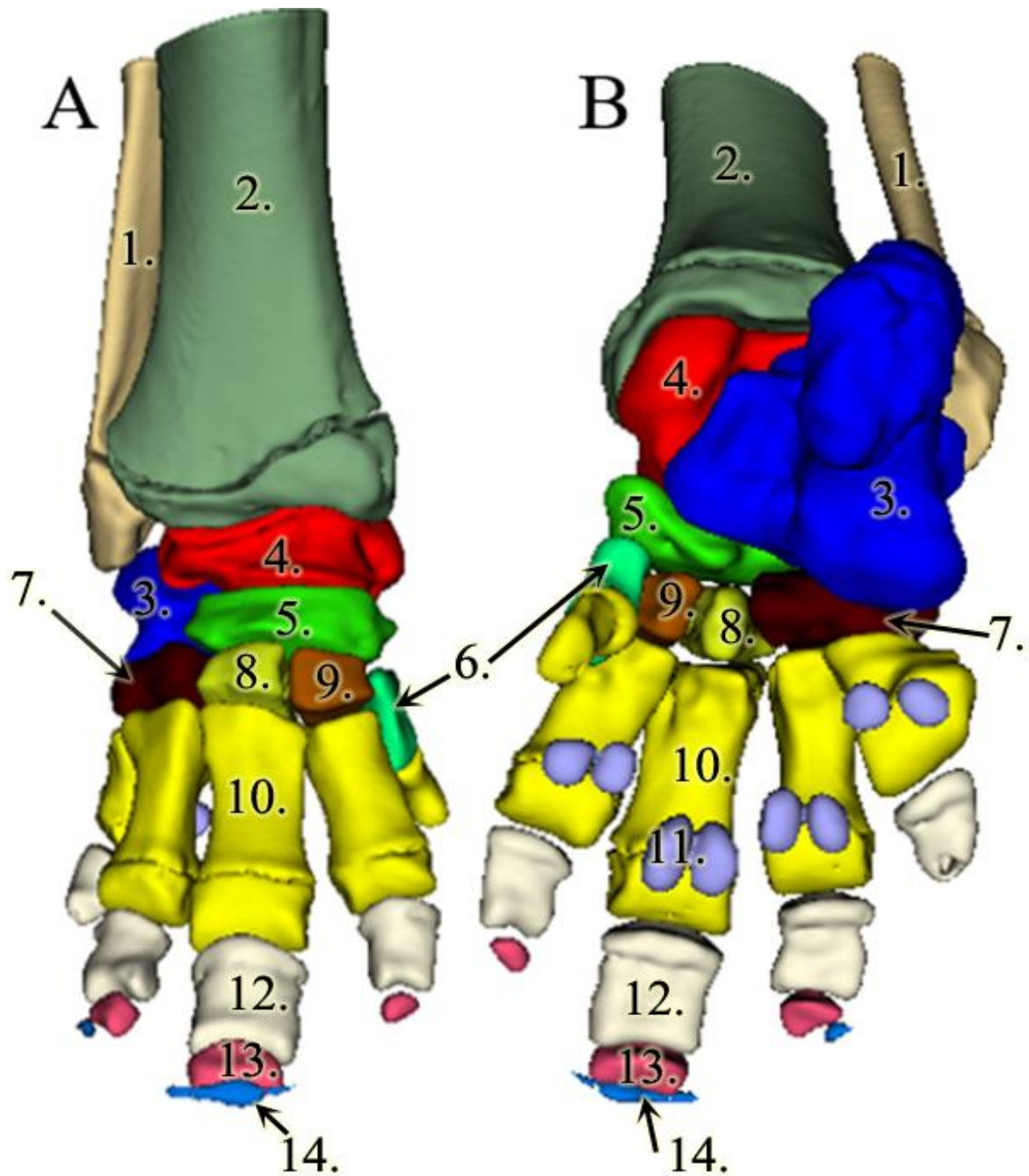


Figure 10.: 3D model of the right hindlimb; **A:** dorsomedial view;

B: distal plantar view.

Crus: **1:** fibula, **2:** tibia.

Tarsus: **3:** calcaneus, **4:** talus, **5:** os tarsi centrale, **6:** os tarsale I, **7:** os tarsale IV,

8: os tarsale III, **9:** os tarsale II.

Metatarsus: **10:** os metatarsale III.

11: ossa sesamoidea proximales (seen in plantar view).

Digiti pedis: **12:** phalanx proximalis III, **13:** phalanx media III,

14: phalanx distalis III.

The positions of the prepollex and prehallux were located with the help of the CT images loaded into the 3D Slicer program (**Figure 11-12.**).

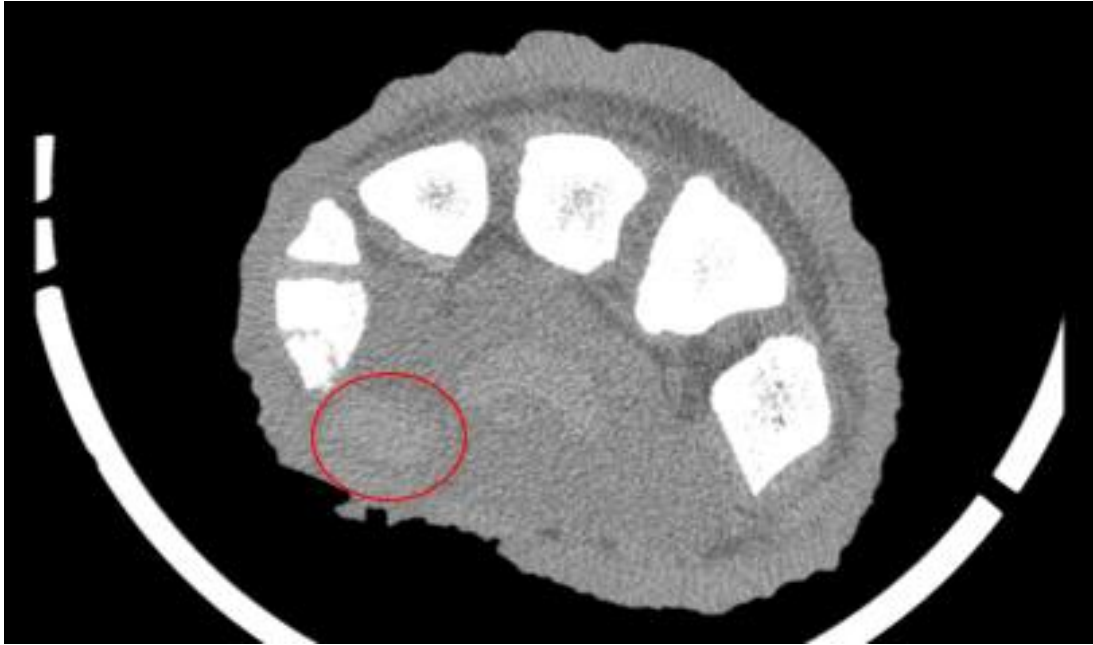


Figure 11.: CT image loaded into 3D Slicer, transverse view of the left forelimb.
Red circle: prepollex

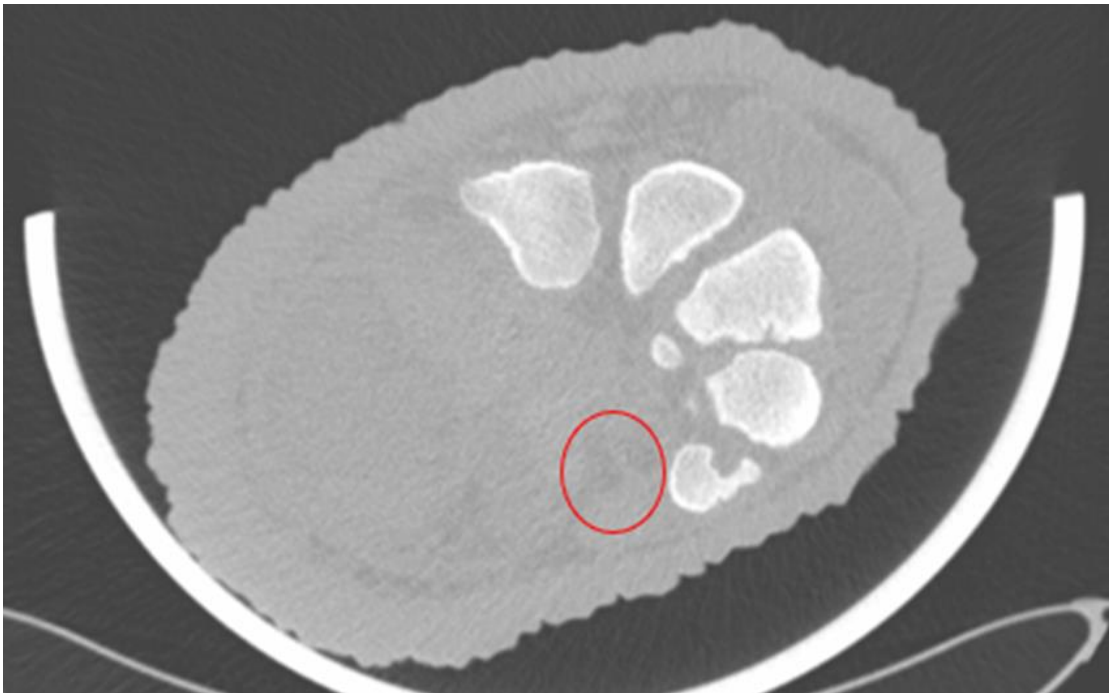


Figure 12.: CT image loaded into 3D Slicer, transverse view of the right hindlimb.
Red circle: prehallux

An additional compilation of the carpal and tarsal bones in different perspectives of the significant characteristics was also developed (**Figures 13-19**).

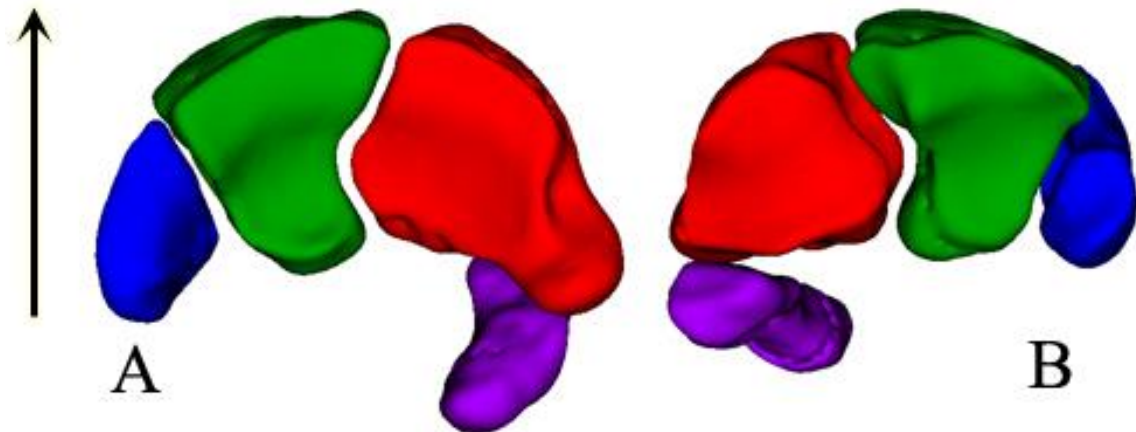


Figure 13.: 3D reconstruction of the left carpal proximal row. The arrow points at the dorsal direction. **A:** distal view. **B:** proximal view. Blue: os carpi radiale, green: os carpi intermedium, red: os carpi ulnare, purple: os carpi accessorium.

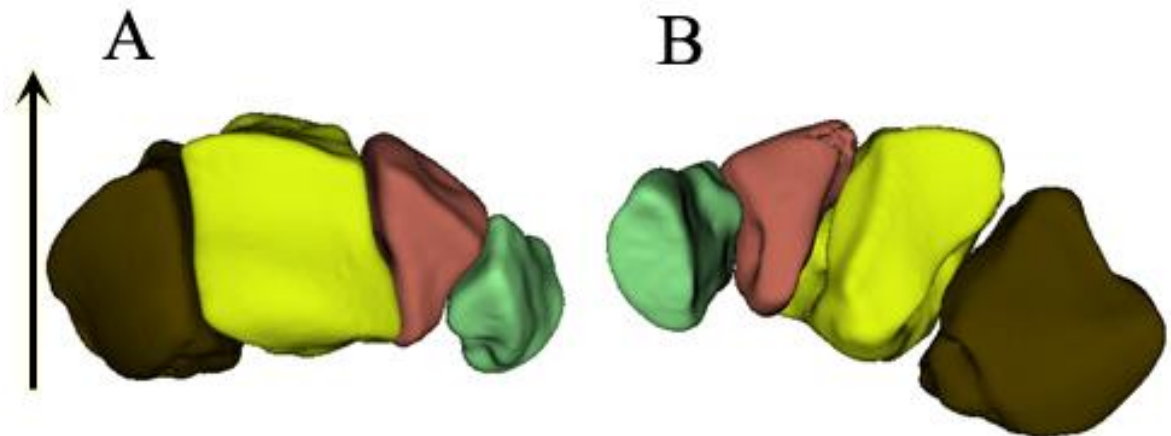


Figure 14.: 3D reconstruction of the left carpal distal row. The arrow points at the dorsal direction. **A:** proximal view. **B:** distal view. Green: os carpale I, teal: os carpale II, yellow: os carpale III, brown: os carpale IV.

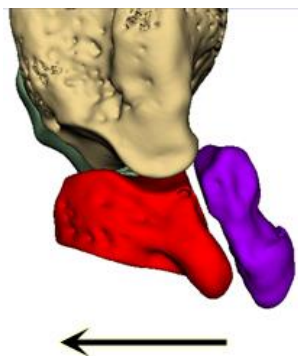


Figure 15.: 3D reconstruction of the left carpal proximal row with the ulna. Lateral view. The arrow points at the dorsal direction. Beige: ulna, red: os carpi ulnare, purple: os carpi accessorium.

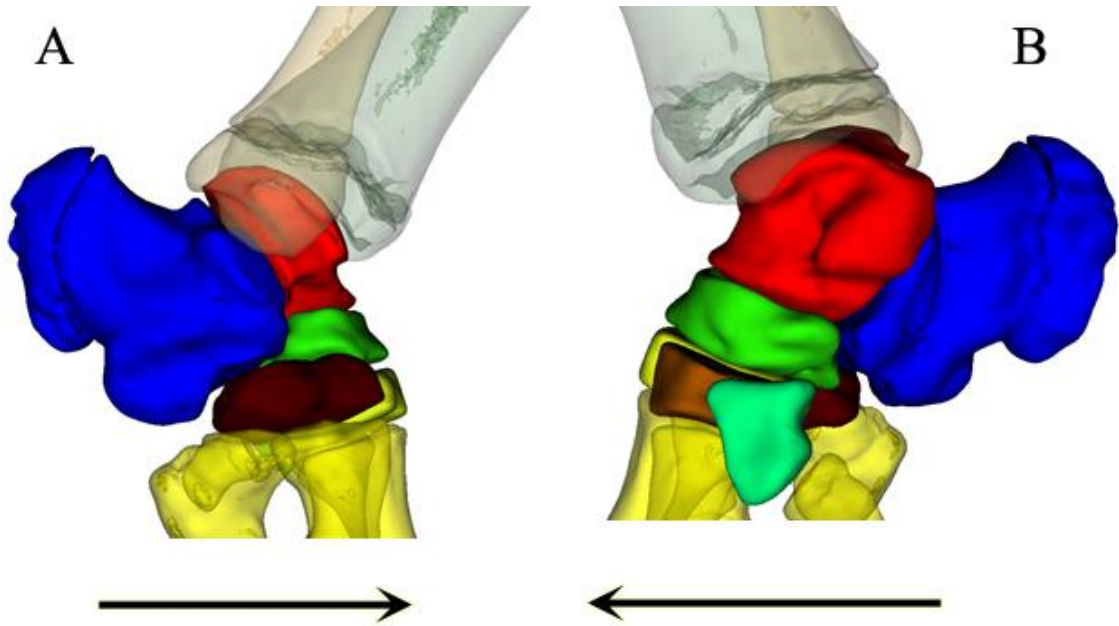


Figure 16.: 3D reconstruction of the right tarsus. Both arrows point at the dorsal direction. The opacity of the tibia, ulna and metatarsal bones is lowered.
A: lateral view. **B:** medial view.

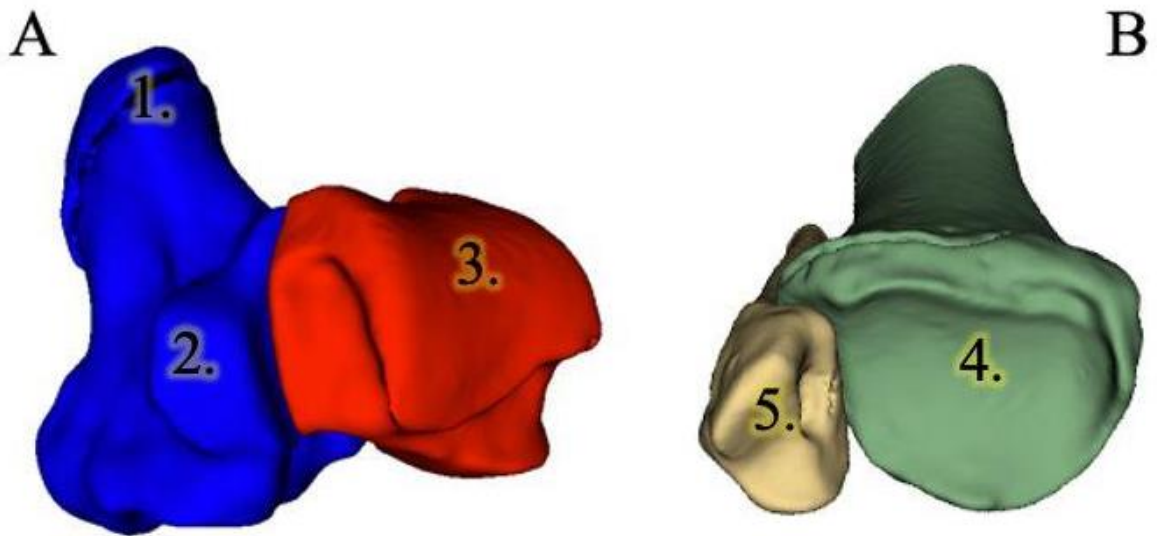


Figure 17.: 3D reconstruction of the matching bone surfaces of the right tarsocrural joint. **A:** dorso-lateral view. **B:** distal view.
 Blue: calcaneus, red: talus, beige: fibula, green: tibia.
 1: tuber calcanei, 2: processus coracoideus, 3: trochlea tali, 4: cochlea tibiae,
 5: facies articularis malleoli.

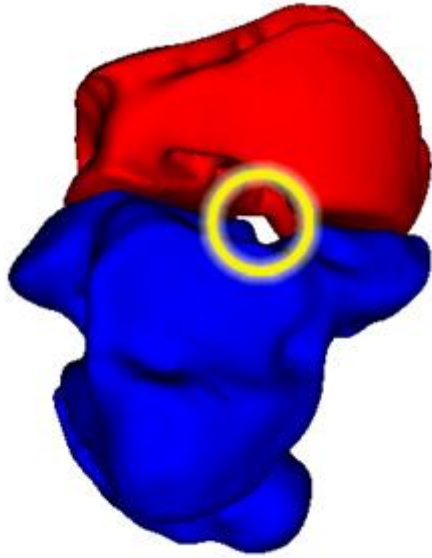


Figure 18.: 3D reconstruction of the bones building the sinus tarsi. Distal view.
Blue: calcaneus, red: talus, yellow circle: sinus tarsi.

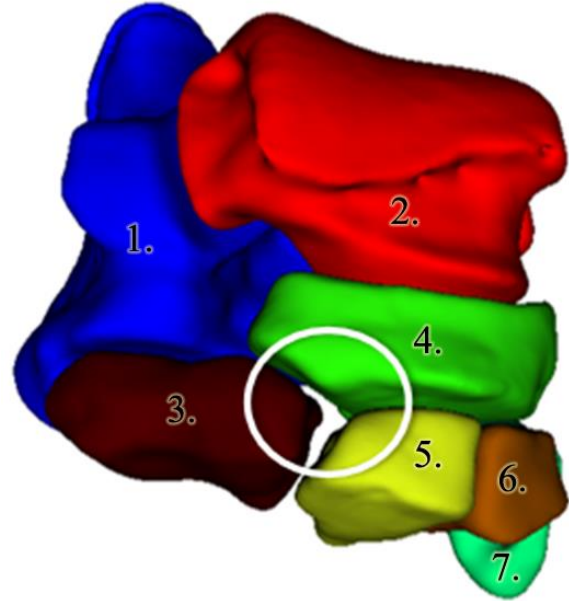


Figure 19.: 3D reconstruction of the tarsus building the canalis tarsi. Dorso-lateral view. 1: calcaneus, 2: talus, 3: os tarsale IV, 4: os tarsi centrale, 5: os tarsale III, 6: os tarsale II, 7: os tarsale I, white circle: canalis tarsi.

4.2. Results of the vessel reconstructions

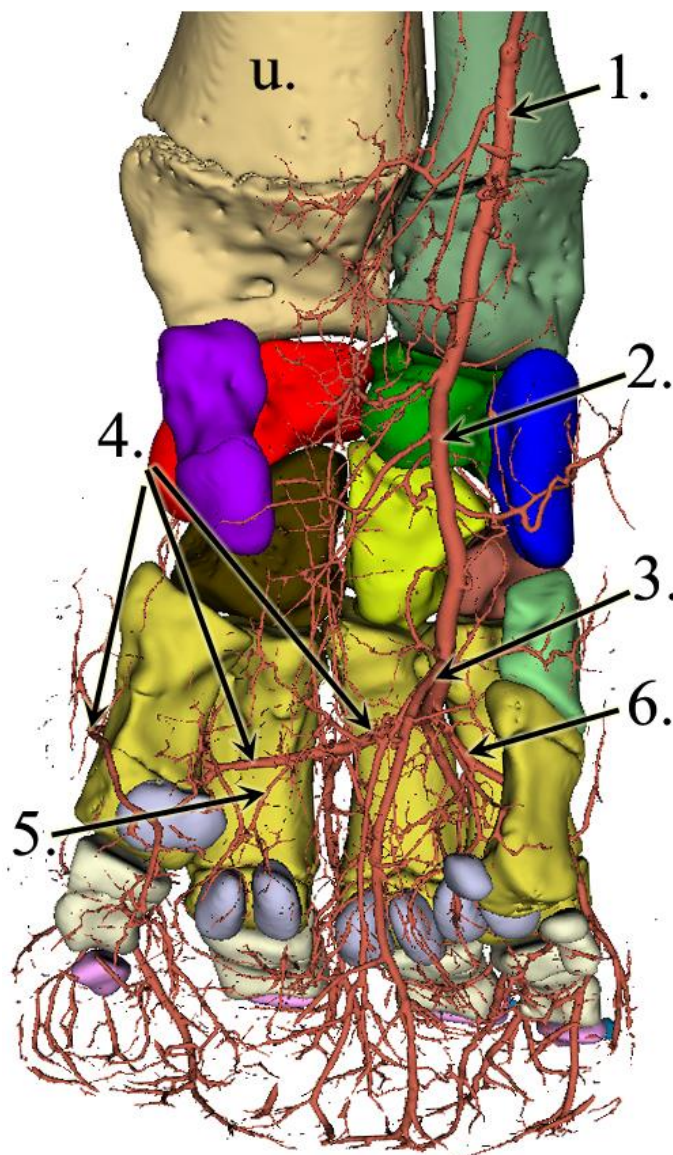
To our knowledge, until today, no 3D models were made of the vessels of an Asian elephant. We were able to create one for the forelimb, displaying the arteries.

We can see the strong *a. mediana* coursing down at the medial aspect of the antebrachium, more exactly on the palmar surface of the radius. At the carpal region, the median artery becomes *a. metacarpea*. There are some small branches supplying the proximal row of the carpus. Additional blood supply for the carpus arise as recurrent branches from the middle dorsal part of the metacarpal bones (**Figure 20.**).

Just before the metacarpal artery becomes the deep palmar arch, we found a major vessel branching off into the palmar direction, that was so far undescribed. The vessel has approximately the same diameter as any of the dorsal metacarpal arteries, it aims distally, and we were able to trace its branches until the level of the sole. It remains close to the median plane of the foot, but a bit closer to the medial side. This vessel runs approximately

8 mm after it emerges, before it develops a trifurcation. The first branch of it turns medially, palmar to the first digit, we assume that it supplies the prepollex as well. The other two branches remain in approximately the same vertical plane, although both are slightly bended into the lateral direction. One of them goes dorsally, the other palmarly and both reach the sole approximately 7-8 cm apart from each other. Close to the sole, the vessels turn towards each other, getting very close, although we cannot confirm an anastomosis, which we think is very likely to happen there (**Figure 21**).

The deep palmar arch bends laterally and runs between the D-IV and D-V before giving up the fourth common digital artery. The terminal section of the deep palmar arch goes



around the fifth metacarpal bone from the dorsal direction, return to the palmar side and gets lost in the lateral side of the digital cushion. The metacarpal arteries that are branching off from the arch become common dorsal digital arteries as they go to the dorsal side between the heads of the corresponding metacarpal bones. These common dorsal digital arteries bear axial and abaxial branches for the neighbouring phalanges (**Figure 22**). Branching off from the deep palmar arch we also located relatively small vessels, the palmar digital arteries, that run on the palmar aspect of the metacarpus before dividing into two and getting lost at the height of the proximal sesamoid bones.

Figure 20.: 3D reconstruction of the forefoots' vessels on the left limb. Palmar view.
1: a. mediana, **2:** a. metacarpea, **3:** newly found vessel, **4:** arcus palmaris profundus, **5:** a. digitalis palmaris IV, **6:** a. metacarpea dorsalis I, **u:** ulna.

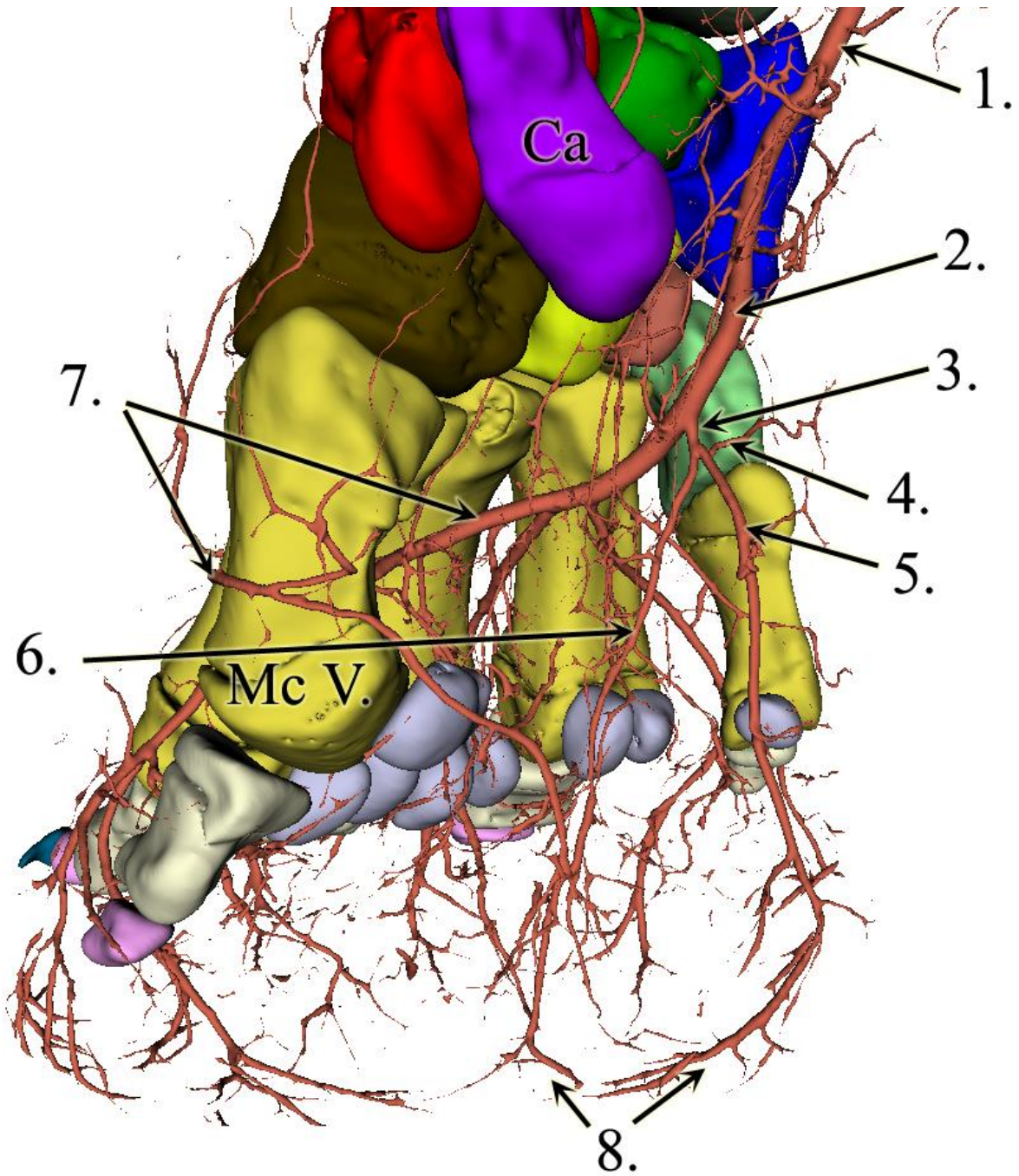


Figure 21.: 3D reconstruction of the forefoot vessels on the left limb.

Latero-palmar view.

1: a. mediana, **2:** a. metacarpea,

3: newly found vessel,

4: branch towards the first digit and prepollex, **5:** palmar branch, **6:** dorsal branch,

7: arcus palmaris profundus,

8: terminal sections of the dorsal and palmar branches headed towards each other in the digital cushion, **Ca:** os carpi accessorium.

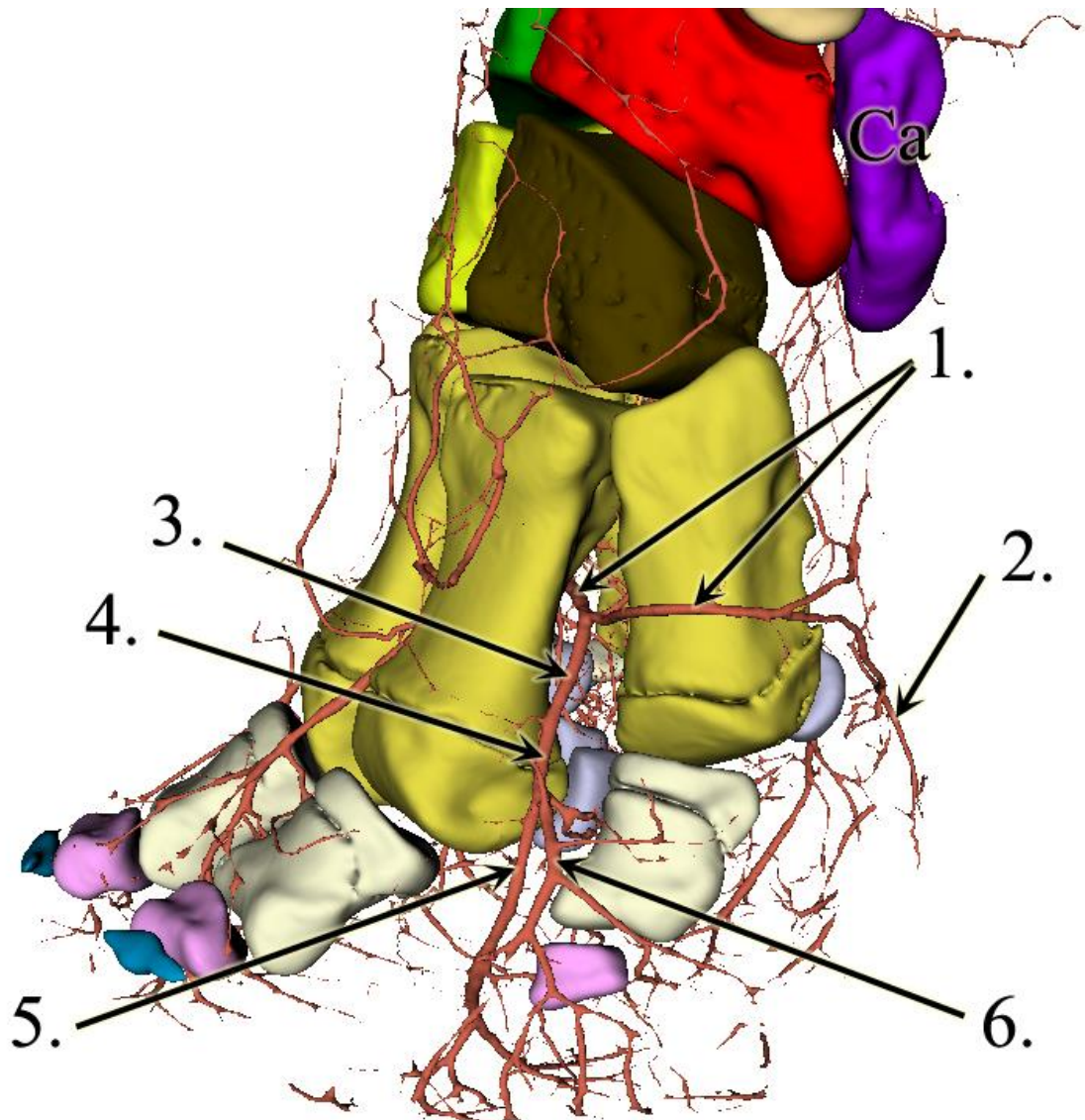


Figure 22.: 3D reconstruction of the forefoot vessels on the left limb.

Lateral view.

1: arcus palmaris profundus, **2:** lateral terminal branch at the dorso-lateral side of the digital cushion, **3:** a. metacarpea dorsalis IV, **4:** a. digitalis dorsalis communis IV,

5: a. digitalis dorsalis IV abaxialis, **6:** a. digitalis dorsalis V axialis,

Ca: os carpi accessorium.

4.3. Results of the joint reconstructions

We were able to fuse the CT and MRI images and to follow the course of cartilages throughout the carpal joint (**Figure 23.**). The cartilages and joint cavities were connected in such a way that we were not able to separate them with our current techniques and settings available. The facet of the cartilages facing the bones were identified and were matched with the corresponding bones originating from the CT reconstruction, but we were not able to securely separate them from the synovia, which was visible only as a thin line (**Figure 24.**).

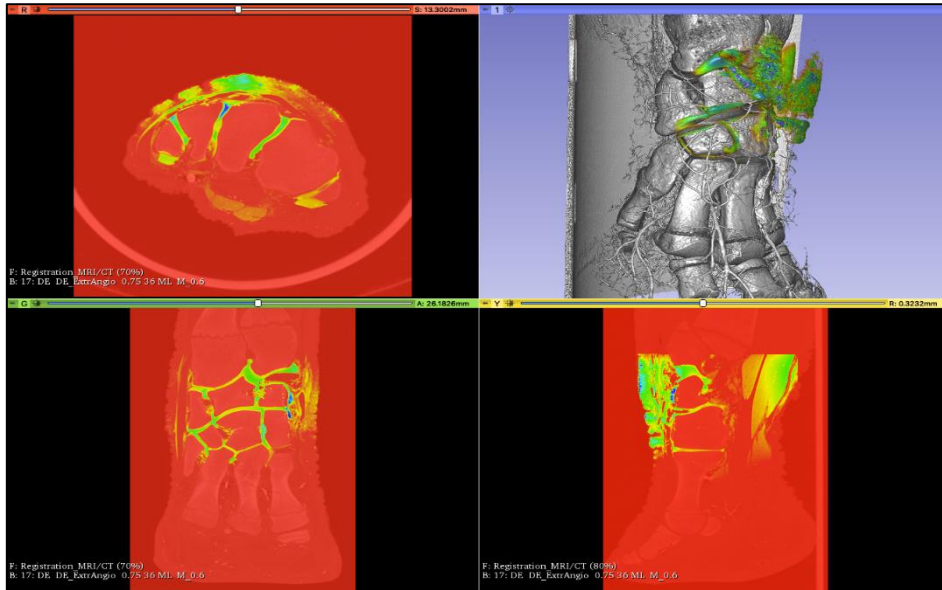


Figure 23.: Screenshot of 3D Slicer; Fused CT and MRI scan with the cartilages of the carpal joint highlighted with neon colours.

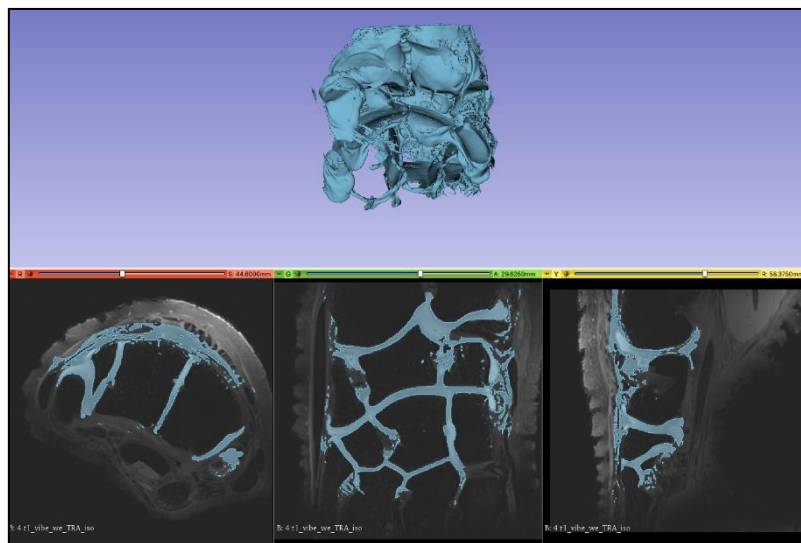


Figure 24.: Screenshot of 3D Slicer with the reconstructed cartilages within the carpal joint cavity.

5. Discussion and conclusion

Anatomy is not always textbook like and that is what makes it so intriguing. The basic knowledge invites for curiosity about which individual subtleties are out there waiting to be found.

In the digits of our specimen we found some aberrations. The forelimbs' first digit is composed of only one phalanx like it is usually in the African elephant, whereas the Asian elephant bears two phalanges on its D-I (**Table 1.**).

Table 1.: Variations and similarities found in the investigated specimens' forelimb compared to known findings, based on Csuti et al. (2001).

| | Investigated specimen | Asian elephant (<i>Elephas maximus</i>) | African elephant (<i>Loxodonta africana</i>) |
|-----------------|-------------------------------------|--|---|
| Forelimb | 5 toenails | 5 toenails | 4 toenails |
| D-I | P-I only | <i>P-I and P-II</i> | P-I only |
| | One single sesamoid bone | One single sesamoid bone | One single sesamoid bone |
| D-II | P-I to P-III | P-I to P-III | P-I to P-III |
| | Paired sesamoid bones | Paired sesamoid bones | Paired sesamoid bones |
| D-III | P-I to P-III | P-I to P-III | P-I to P-III |
| | Paired sesamoid bones | Paired sesamoid bones | Paired sesamoid bones |
| D-IV | P-I to P-III | P-I to P-III | P-I to P-III |
| | Paired sesamoid bones | Paired sesamoid bones | Paired sesamoid bones |
| D-V | P-I and P-II | P-I and P-II | P-I and P-II |
| | Paired sesamoid bones, fused | Paired sesamoid bones | Paired sesamoid bones |

Furthermore, on the hindlimb we recognized certain variations as well (**Table 2.**). In the first digit of the hindlimb no phalangeal structures are found, the MT-I is the most distal bone here. That does not correlate with neither the African who bears even two phalanges nor with the Asian with at least one phalanx. D-II consists of only the first phalanx, like it would be in the African elephant, the Asian species has a proximal and intermediate phalanx in place. The fifth digit of our specimen bears only one phalanx, whereas both the African and Asian elephant have usually two phalanges here. We can say that our specimen shows similarities with both species' characteristics, and some structures are completely different. It shows that even within a species we always can expect differences to a certain extent.

Table 2.: Variations and similarities found in the investigated specimens' hindlimb compared to known findings, based on Csuti et al. (2001).

| | Investigated specimen | Asian elephant (<i>Elephas maximus</i>) | African elephant (<i>Loxodonta africana</i>) |
|-----------------|--------------------------------|--|---|
| Hindlimb | 4 toenails | 4 toenails | 3 toenails |
| D-I | MT-I (no phalanges) | <i>P-I only</i> | P-I and P-II |
| | No sesamoid bone | No sesamoid bone | No sesamoid bone |
| D-II | P-I and P-II | <i>P-I to P-III</i> | P-I and P-II |
| | Paired sesamoid bones | Paired sesamoid bones | Paired sesamoid bones |
| D-III | P-I to P-III | P-I to P-III | P-I to P-III |
| | Paired sesamoid bones | Paired sesamoid bones | Paired sesamoid bones |
| D-IV | P-I to P-III | P-I to P-III | P-I to P-III |
| | Paired sesamoid bones | Paired sesamoid bones | Paired sesamoid bones |
| D-V | P-I only | <i>P-I and P-II</i> | P-I and P-II |
| | Paired sesamoid bones | Paired sesamoid bones | Paired sesamoid bones |

These individual differences are not rare in elephants, where multipartite, missing or misshapen phalanges as well as multiple variations of the proximal sesamoid bones (fused together, as a pair or completely missing) can be frequent adverse findings in clinical radiographs or CT scans (Regnault et al., 2017). The number of toenails were in line with the usual findings in the Asian elephants and were in a good condition as far as we could evaluate this from the reconstructions. The condition of the toenails can be a significant indicator for the overall foot health and may suggest underlying abnormal bone confirmations (Luikart & Stover, 2005).

Based on our results, we can confirm that the tarsus of the elephant bears a *sinus tarsi*, build up from the *sulcus tali* and *sulcus calcanei*. The literature already mentioned articular surfaces between the calcaneus and the talus, but no further details on them were described. Additionally, the *canalis tarsi* could be demonstrated in the 3D model, formed by the os tarsi centrale, os tarsale III and IV.

The prepollux and prehallux in our specimen were completely unossified because the 3D Slicer did not identify and therefore did not colour them coevally with the bones. The image settings were not appropriate for a definite identification of the sixth digits, but on the CT scans of the fore-and hindlimb a shadow at the proper place – at the distal end of C-I/T-I and the proximal end of MC-I/MT-I – can be presumed as the prepollux and prehallux. These findings conform with previous investigations, where the predigits showed various appearances, they can stay cartilaginous, become partly ossified or completely ossified during an elephants' life (Hutchinson et al., 2011; Miller et al., 2008; Regnault et al., 2017).

The distal growth plates of the antebrachium and crus were opened, as well as the proximal growth plates on the proximal phalanges (P-I) of the forefoot and the distal growth plates on the metacarpal and metatarsal bones. This is in line with the age of our subject, as these growth plates would only close by 9-10 years of age (Siegal-Willott et al., 2008).

For the reconstruction of the vessels, we could not find other visual materials for comparison, just a few written explanations. We were able to obtain suitable images of the vessels of the forelimb and discovered some interesting features. We found a vessel which was most likely not described until now, which runs in the direction of the digital cushion (*torus digitalis*). Similar branches were mentioned in other ungulates like ruminants and horses before, namely the *rr. tori digitales* for the supply of the footpads. These branches exist usually as paired (abaxial/axial or lateral/medial) branches per limb, but discharge from much more distal arteries like the *a. coronalis* or the *aa. digitales palmares propriae*

(Constantinescu et al., 2012; Nickel et al., 2005). Our vessel divides into two portions as well, but into dorsal and palmar directions. A reason therefore could be the different foot setup (semidigitigrade versus unguligrade) or the huge extent of the cushion. Despite the fact that we only had the opportunity to examine one single specimen, it is absolutely logical that in elephants homologous vessels exist, as the digital cushion plays an important role for the weight compensation of these massive animals.

As this vessel runs into the direction of the digital cushion, and if it is the case that it supplies it, we suggest the name *a. tori digitalis communis* until the trifurcation, where for the three vessels we suggest *r. dorsalis*, *r. palmaris* and *r. digitalis I*. We did not find the branch of the metacarpal artery that goes to the first digit which was mentioned in the literature, but the *r. digitalis I* could be an alternatively flowing branch. We could not find the interosseus branch of the median artery, but it is possible that this branch goes off from the median artery at a position proximal to where the forelimb cut, or the BaSO₄ was not able to enter this vessel because it was damaged during the cutting process. Another so far undescribed feature of the vessels is that the *arcus palmaris profundus* runs between the fourth and fifth metacarpal and turns over to the dorsal aspect of the fifth metacarpal bone before returning to the palmar side, with its terminal section supplying the digital cushion. As we only examined one animal, which even had some deviations in the number of the phalanges, we cannot declare that our discovery is definitely more than an individual finding, but as similar vessels exist in many other species, it was expectable to have a significant vessel for this purpose in this region. We were not able to reconstruct the hindlimbs' vessels in this investigation due to technical problems. Most probably the hindlimb was cut too deep, therefore it was difficult to locate and then to inject a proper amount of the contrast medium into the vessels.

We successfully fused the CT and MRI images, and we could colour the cartilages, but were not able to reliably follow the joint cavity wall or separate them nicely from the surrounding connective tissue. The separate illustration was not realisable with our current methods; thus, we made the decision to focus on the detailed bone and vessel description. For more distinctive results more specific investigations and techniques should be applied.

Maybe if the opportunity is there, further investigations with the arteries and veins combined could be made to see their courses throughout the limbs. Regarding our efforts with the hindlimbs' vessel, the suggestion can be made to cut a specimen more proximally, before the *a. poplitea* divides into the cranial and caudal tibial arteries, so that the chance to

find it and to be able to inject a proper amount of contrast medium is much higher. It is advisable as well to use enough contrast medium to get the full course of even small branches better.

Because our specimen belongs to an endangered species, we had limited opportunities to examine the limbs. We could not use more accurate techniques like cryosectioning (Czeibert et al., 2019), which would lead consequently to the destruction of the limbs. For the same reason we were not allowed to further dissect the limb or to build a specimen of any kind, such as a skeleton, for educational purposes.

Nevertheless, during our investigations and with the methods we used, especially with the combination of CT imaging and reconstruction with a program such as the 3D Slicer, we were able to find the anatomical structures we wanted to present and highlight unique individual anatomical differences, which were not described before in the Asian elephant. We created valuable 3D models of the bones and vessels, which can be used for 3D printing as well, accessible for everyone who is interested in the topic.

6. Summary

3D reconstruction and analyses of the anatomy of an elephant's foot using CT and MRI

Being the largest still living terrestrial mammal on earth, elephants have always played an important role in an economical, social and ecological point of view. The Asian elephant (*Elephas maximus*) is listed on the Red List as a highly endangered species, indicating its steadily declining population. Therefore, it is even more important to preserve these animals and to ensure their good health. Elephant's feet play an important role in their health status, because their high body weight is supported by them, which resulted in many interesting features in the anatomy. The aim of this work is to provide anatomical guidance of structures found in the feet, focusing on bones, the vasculature and joints.

The Somogy County Kaposi Mór Teaching Hospital, Dr. Baka József Diagnostical and Oncoradiological Centre got the opportunity to examine a front- and hindlimb of a deceased 6-year old female Asian elephant by CT and MRI, where over 5.000 CT and 300 MRI images were recorded. First native sequences were taken, then the arteries were filled with iodine containing contrast media and the CT scans were repeated in the same position. The resulting data were processed with the 3D Slicer software. After quality evaluation of the obtained sequences, one series of each CT and MRI was chosen for the 3D reconstruction of the bones, vessels and joint cavities.

Literature already exists about the anatomy of the feet, but only few 3D data can be found, which does not include the vessels and joint cavities. Our results and 3D reconstructions, which will be accessible online as well and can even be 3D printed for further demonstration, will help to understand the complex anatomy of elephant's feet. It can be utilized in many fields, especially by veterinarians, students and keepers.

7. Összefoglaló

Az elefánt lábvégének CT és MRI alapú 3D rekonstrukciós vizsgálata

A legnagyobb szárazföldi emlősként az elefánt mindig is kiemelkedő gazdasági, szociális és ökológiai szerepet töltött be. Az ázsiai elefánt (*Elephas maximus*) populációjának folyamatosan csökkenő létszámát jelzi, hogy a veszélyeztetett fajokat felsoroló ún. Vörös Listán is szerepel. Emiatt különösen fontos, hogy ezen állatokat minél inkább megóvjuk és jó egészségben tartsuk. Az elefántok lába különösen fontos az általános egészségi állapotuk szempontjából, mert ezek viselik a test hatalmas tömegét, így rengeteg egyedi anatómiai képlettel rendelkeznek. Munkánk során, a keresztmetszeti képalkotó módszereket felhasználva, az elefánt lábvég csontjait, artériáit és ízületeit is magában foglaló 3D rekonstrukciókat és modelleket készítettük el volt.

A Somogy Megyei Kaposi Mór Oktató Kórház, Dr. Baka József Diagnosztikai és Onkoradiológiai Központjában egy természetes okokból elhullott 6 éves, nőtény ázsiai elefánt mellső és hátulsó lábának CT és MRI vizsgálatára nyílt lehetőség, amelyekről összesen több, mint 5.000 CT és 300 MR felvétel készült. Először natív szekvenciák készültek, majd az artériás rendszer jód- tartalmú kontrasztanyaggal való feltöltése után a CT felvételeket megismételtük. A kapott szekvenciákat a 3Dslicer szoftverrel dolgoztuk fel. A képsorozatok kiértékelése után a legalkalmasabbakon rekonstruáltuk a csontokat, ereket és az ízületek üregeit.

Az elefánt lábvég anatómiájának létezik ugyan valamennyi irodalma, de minimális 3D adat elérhető, ami nem terjed ki az erekre és az ízületekre. Az elkészített rekonstrukciós modellek online is elérhetőek lesznek, valamint 3D nyomtatással kézzelfogható készítményként is használhatóak, segítséget nyújtanak az elefánt komplex anatómiájú lábvégének a megértésében. Munkánk így nagyon sok területen, különösen állatorvosok, hallgatók és állattartók számára lesz hasznosítható.

8. Bibliography

- Ahasan, A.S.M.L, Quasem, M.A., Rahman, M.L., Hasan, R.B., Kibria, A.S.M.G., Shil, S.K., 2016: Macroanatomy of the Bones of Thoracic Limb of an Asian Elephant (*Elephas maximus*). *International Journal of Morphology*, 34(3), 909–917.
- Csuti B., Sargent E.L., Bechert U.S., 2001: The elephant's foot - Prevention and Care of Foot Conditions in Captive Asian and African Elephants. Iowa State University Press, Ames.
- Czeibert, K., Baksa, G., Grimm, A., Nagy, Sz.A., Kubinyi, E., Petneházy, Ö., 2019: MRI, CT and high resolution macro-anatomical images with cryosectioning of a Beagle brain: Creating the base of a multimodal imaging atlas. *PLOS ONE*, 14. e0213458.
- Constantinescu, G., Habel, R., Hillebrand, A., Sack, W., Schaller, O., Simoens, P., De Vos, N., 2012: Illustrated Veterinary Anatomical Nomenclature. 3rd ed. Stuttgart: Enke.
- Fedorov A., Beichel R., Kalpathy-Cramer J., Finet J., Fillion-Robin J-C., Pujol S., Bauer C., Jennings D., Fennessy F., Sonka M., Buatti J., Aylward S.R., Miller J.V., Pieper S., Kikinis R., 2012: 3D Slicer as an Image Computing Platform for the Quantitative Imaging Network. *Magnetic Resonance Imaging*. 30(9):1323-41.
- Fowler M.E., Mikota S.K., 2006: Biology, Medicine and Surgery of Elephants, 1st ed. Blackwell, Ames.
- Hutchinson, J.R., Delmer, C., Miller, C.E., Hildebrandt, T., Pitsillides, A.A., Boyde, A., 2011: From flat foot to fat foot: Structure, ontogeny, function, and evolution of elephant "sixth toes". *Science*, 334(6063), 1699–1703.
- IUCN (International Union for Conservation of Nature and Natural Resources), 2020: The IUCN Red List of Threatened Species, Version 2020-2.
URL: <https://www.iucnredlist.org>, Last accessed: 23.10.2020, 20:49.
- Kapur, T., Pieper, S., Fedorov, A., Fillion-Robin, J.-C., Halle, M., O'Donnell, L., Lasso, A., Ungi, T., Pinter, Cs., Finet, J., Pujol, S., Jagadeesan, J., Tokuda, J., Norton, I., Estepar, R.S.J., Gering, D., Aerts, H.J.W.L., Jakab, M., Hata, N., Ibanez, L., Blezek, D., Miller, J., Aylward, S., Grimson, W.E.L., Fichtinger, G., Wells, W.M., Lorensen, W.E., Schroeder, W., Kikinis, R., 2016: Increasing the Impact of Medical Image Computing Using Community-Based Open-Access Hackathons: The NA-MIC and 3D Slicer Experience. *Medical Image Analysis* 33 (October): 176–80.
- Kellogg, M. E., Burkett, S., Dennis, T. R., Stone, G., Gray, B. A., McGuire, P. M., Zori, R. T., Stanyon, R., 2007: Chromosome painting in the manatee supports Afrotheria and Paenungulata. *BMC Evolutionary Biology*, 7 (clade I), 1–7.
- Kikinis R., Pieper S.D., Vosburgh K., 2014: 3D Slicer: a platform for subject-specific image analysis, visualization, and clinical support. *Intraoperative Imaging Image-Guided Therapy*, Ferenc A. Jolesz, Editor 3(19):277–289.
- Larramendi, A., 2016: Shoulder height, body mass, and shape of proboscideans. *Acta Palaeontologica Polonica*, 61(3), 537–574.

- Luikart, K.A., Stover, S.M., 2005: Chronic sole ulcerations associated with degenerative bone disease in two Asian elephants (*Elephas maximus*). *Journal of Zoo and Wildlife Medicine*, 36(4), 684–688.
- Miller, C.E., Basu, C., Fritsch, G., Hildebrandt, T., Hutchinson, J.R., 2008: Ontogenetic scaling of foot musculoskeletal anatomy in elephants. *Journal of the Royal Society Interface*, 5(21), 465–475.
- Mumby, C., Bouts, T., Sambrook, L., Danika, S., Rees, E., Parry, A., Rendle, M., Masters, N., Weller, R., 2013: Validation of a new radiographic protocol for Asian elephant feet and description of their radiographic anatomy. *Veterinary Record*, 173(13), 318.
- Nickel R., Schummer A., Seiferle E., 2005: *Lehrbuch der Anatomie der Haustiere. Band III. Kreislaufsystem, Haut und Hautorgane.* Verlag Paul Parey, Stuttgart.
- Regnault, S., Dixon, J.J., Warren-Smith, C., Hutchinson J.R., Weller, R., 2017: Skeletal pathology and variable anatomy in elephant feet assessed using computed tomography. *PeerJ* 5:E2877.
- Weissengruber, G.E., Egger, G.F., Hutchinson, J.R., Groenewald, H.B., Elsässer, L., Famini, D., Forstenpointner, G., 2006: *The structure of the cushions in the feet of African elephants (Loxodonta africana)*. 781–792.
- Siegal-Willott, J., Isaza, R., Johnson, R., Blaik, M., 2008: Distal limb radiography, ossification, and growth plate closure in the juvenile Asian elephant (*Elephas maximus*). *Journal of Zoo and Wildlife Medicine*, 39(3), 320–334.
- Smuts, M.M.S, Bezuidenhout, A.J., 1993: Osteology of the thoracic limb of the African elephant (*Loxodonta africana*). *Onderstepoort Journal of Veterinary Research*, 60:1-14.
- Smuts, M.M.S, Bezuidenhout, A.J., 1994: Osteology of the pelvic limb of the African elephant (*Loxodonta africana*). *Onderstepoort Journal of Veterinary Research*, 61:51-66.

9. Acknowledgements

I would like express my sincere thanks to the Somogy County Kaposi Mór Teaching Hospital, Dr. Baka József Diagnostical and Oncoradiological Centre and the specialists of Medicopus Nonprofit Ltd. for the CT and MRI images with which we could create these beautiful images and 3D models.

Huge thanks to both of my supervisors: Dr. Reinitz László Zoltán for being always there for advice while writing this thesis, taking his time for every of his students to get the best result possible and Dr. Petneházy Örs, who introduced me to the world of 3D reconstructions and made it possible that we get such great reconstructions.

Thanks to the head of the department and dean of the University Dr. Sótonyi Péter and the whole Department of Anatomy and Histology, which allowed me to perform the thesis with them.

Thanks to Lassó András, who helped in any issues regarding the 3D Slicer.

Last, but not least I want to express my deep gratefulness to my beloved ones, my parents, friends and partner who are always there to support me and who are always by my side.

HuVetA

ELECTRONIC LICENSE AGREEMENT AND COPYRIGHT DECLARATION*

Name: Rück, Shannon

Contact information (e-mail): shannon.rueck@web.de

Title of document (to be uploaded): 3D reconstruction and analyses of the anatomy of an elephant's foot using CT and MRI

Publication data of document: TDK

Number of files submitted: 1

By accepting the present agreement the author or copyright owner grants non-exclusive license to HuVetA over the above mentioned document (including its abstract) to be converted to copy protected PDF format without changing its content, in order to archive, reproduce, and make accessible under the conditions specified below.

The author agrees that HuVetA may store more than one copy (accessible only to HuVetA administrators) of the licensed document exclusively for purposes of secure storage and backup, if necessary.

You state that the submission is your original work, and that you have the right to grant the rights contained in this license. You also state that your submission does not, to the best of your knowledge, infringe upon anyone's copyright. If the document has parts which you are not the copyright owner of, you have to indicate that you have obtained unrestricted permission from the copyright owner to grant the rights required by this Agreement, and that any such third-party owned material is clearly identified and acknowledged within the text of the licensed document.

The copyright owner defines the scope of access to the document stored in HuVetA as follows (**mark the appropriate box with an X**):

- I grant unlimited online access,
- I grant access only through the intranet (IP range) of the University of Veterinary Medicine,
- I grant access only on one dedicated computer at the Ferenc Hutýra Library,
- I grant unlimited online access only to the bibliographic data and abstract of the document.

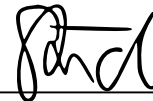
Please, define the **in-house accessibility of the document** by marking the below box with an **X**:

I grant in-house access (namely, reading the hard copy version of the document) at the Library.

If the preparation of the document to be uploaded was supported or sponsored by a firm or an organization, you also declare that you are entitled to sign the present Agreement concerning the document.

The operators of HuVetA do not assume any legal liability or responsibility towards the author/copyright holder/organizations in case somebody uses the material legally uploaded to HuVetA in a way that is unlawful.

Date: Budapest, 25.10.2020



Author/copyright owner
signature

HuVetA Magyar Állatorvos-tudományi Archívum – Hungarian Veterinary Archive is an online veterinary repository operated by the Ferenc Hutýra Library, Archives and Museum. It is an electronic knowledge base which aims to collect, organize, store documents regarding Hungarian veterinary science and history, and make them searchable and accessible in line with current legal requirements and regulations.

HuVetA relies on the latest technology in order to provide easy searchability (by search engines, as well) and access to the full text document, whenever possible.

Based on the above, HuVetA aims to:

- *increase awareness of Hungarian veterinary science not only in Hungary, but also internationally;*
- *increase citation numbers of publications authored by Hungarian veterinarians, thus improve the impact factor of Hungarian veterinary journals;*
- *present the knowledge base of the University of Veterinary Medicine Budapest and its partners in a focussed way in order to improve the prestige of the Hungarian veterinary profession, and the competitiveness of the organizations in question;*
- *facilitate professional relations and collaboration;*
- *support open access.*